Contents lists available at ScienceDirect

Journal of Industrial and Engineering Chemistry

Pore size distribution control of pitch-based activated carbon for improvement of electrochemical property

Eun-sam Cho [a,b], Byong Chol Bai [a], Ji Sun Im [a,c,*], Chul Wee Lee [a,c], Seok Kim [b,*]

[a] C-Industry Incubation Center, Korea Research Institute of Chemical Technology (KRICT), Daejeon 305-600, Republic of Korea
[b] Department of Chemical and Biomolecular Engineering, Pusan National University, Busan 609-735, Republic of Korea
[c] University of Science and Technology (UST), Daejeon 305-333, Republic of Korea

ABSTRACT

Activated carbon has been prepared using coal tar pitch as a precursor with a simple NaOH activation process. The effect of the activation on the porosity and the specific surface area is characterized by nitrogen adsorption–desorption isotherms. The highest specific surface area of $1409.7 \, \mathrm{m^2 \, g^{-1}}$ is obtained with a NaOH to pitch ratio of 6. Its specific capacitance is $287.43 \, \mathrm{F \, g^{-1}}$ at the scan rate $50 \, \mathrm{mV \, s^{-1}}$, $197.78 \, \mathrm{F \, g^{-1}}$ at the current density $1 \, \mathrm{A \, g^{-1}}$, and it has outstanding energy density of $16.34 \, \mathrm{Wh \, kg^{-1}}$. Thus, pitch-based AC is a promising material for various energy storage devices.

© 2016 The Korean Society of Industrial and Engineering Chemistry. Published by Elsevier B.V. All rights reserved.

Introduction

International Union of Pure and Applied Chemistry (IUPAC) defines pitch as the residue obtained after pyrolysis of organic materials or distillation of tar [1]. It is also means that pitch is a complex form consisting of aromatic hydrocarbons and heterocyclic compounds.

Pitch obtained from coal tar or petroleum. Both pitch types are complex mixtures of organic molecules that primarily consist of polycyclic aromatic hydrocarbons (PAH) [2]. This polycyclic aromatic structure of pitches results in isotropic or anisotropic semicokes formation during heat treatment processes. Due to this chemical property of pitches, main applications rely on their chemical characteristic structure.

Commercially, petroleum and coal-tar pitches turned from worthless wastes into important raw materials of carbonaceous materials. Manufacturing of graphite electrodes, carbon fibers, carbon–carbon composites, activated carbons, and mesophase carbon fibers can be obtained by pyrolysis and carbonization processes of pitch [3,4], and this conjugation can create a high added value.

Electrochemical capacitors (ECs) are energy storage devices that expected as a secondary electric power supplier for the automobiles with hybrid engine or fuel cell motor due to their high power density, long cycle life and short charge time [5]. However, compared with usual batteries, electrochemical capacitors have much lower energy densities. In order to overcome this shortage and to improve the performance of capacitor, the selection of electrode materials is important.

Electrical double layer capacitors (EDLCs) use carbonaceous materials such as carbon aerogels, carbon fibers, graphite, and activated carbons obtains by physical activation or chemical activation from different precursors [6]. As EDLCs stores the electric power by adsorbing electrolyte ions at the interface between electrode and electrolyte, the activated carbon (AC) having properties that high specific surface area and porous structure has been considered as an electrode material for EDLCs among the many types of active materials, without doubt.

Generally speaking, the higher surface area of the electrode, the more energy can be stored because of much electrochemical reaction sites [7,8]. Strictly speaking, but relationship between the specific capacitance and total surface area is not clearly linear [9]. The pore size distribution plays a crucial role in the performance of EDLCs, because surface of micropores must be accessible to electrolyte ions and a suitable amount of mesopores help a rapid mass transport of ions within the electrode enabling

---

* Corresponding author. Tel.: +82 1028556644; fax: +82 428607366.
E-mail address: jsim@krict.re.kr (J.S. Im).

the charging and discharging the double layer [10]. Therefore, an appropriate ratio of micropore and mesopore leads to an improved capacitance.

In this study, coal tar pitch was used as the precursor of activated carbon for electrode of EDLC. The pitch-based activated carbon by NaOH has advantages that a low cost, well developed porous structure, and high activation yield. A series of activated carbon from pitch using NaOH of various amounts was prepared to understand the relationship between porosity characteristics and electrochemical properties.

Experimental details

Materials

Coal tar pitch (purchased from Ansan Co., SN-280#), was used as the raw material to prepare ACs. Pitch has carbon content of 90–93 wt% and ash content of 0.1%. Softening point is 280 °C. Sodium hydroxide (NaOH, bead, 98%, Samchun Co.) was sued as a chemical agent for activation.

Chemical activation of coal tar pitch

The activation of coal tar pitch was carried out by NaOH at 750 °C for 3 h under N_2 flow in tube furnace. The NaOH/Pitch weight ratio (control variable) was 1, 2, 4, and 6. The obtained ACs were washed with distilled water several times, and dried at 100 °C in vacuum oven (MVP 12, Woosung Vacuum Co., 5×10^{-4} torr) for overnight. The prepared ACs were denoted as AC1, AC2, AC4, and AC6 (named by NaOH/Pitch weight ratio).

Morphology and structure analyses

The crystalline structure of the samples was determined by a X-ray diffraction (XRD) analysis (D8, Germany) with Cu Kα (λ = 1.54056 Å).

Fourier transform infrared spectrometry (FT-IR) was carried out with a Spectrum GX over the wavenumber range of 4000–400 cm^{-1}.

Nitrogen adsorption analysis was conducted at 77 K to examine the changes in the specific surface areas and pore structures of the pitch-based activated carbon by NaOH activation.

The specific surface area and the total pore volume were calculated using the Brunauer–Emmett–Teller (BET) equation. The micropore volume was calculated using the Dubinin–Radushke-vitch (D–R) equation, and the pore volumes of the mesoporous were investigated according to the Barrett–Joyner–Halenda (BJH) method. The pore size distribution was calculated using the density functional theory (DFT).

The microstructures of the samples were investigated using field emission scanning electron microscopy (Tescan Mira 3 LMU FEG).

Electrochemical measurements

Electrochemical measurement such as cyclic voltammetry (CV) and Galvanostatic charge–discharge was carried out on potentio-stat/galvanostat (IviumStat, Netherland) in a potential window from −0.9 to 0.0 V in 6 M KOH electrolyte. The three electrodes test cell was composed of nickel foam as a working electrode, saturated calomel electrode (SCE) as a reference electrode, and platinum wire as a counter electrode. The working electrode was prepared by mixing pitch-based activated carbon, carbon black, and polyvi-nylidene fluoride (PVDF) in a mass ratio of 85:10:5 with a small amount (3–5 ml) of N-methyl-2-pyrrolidone (NMP) solvent. The prepared mixture was pasted onto nickel foam (1 cm × 1 cm)

current collector, and dried in oven at 100 °C for 12 h to remove solvent.

Results and discussion

Material characterization

XRD patterns of the pitch-based activated carbon samples are shown in Fig. 1. NaOH-activated carbon appeared a relatively strong peak at 26° and this result indicated that the activated carbon had (002) crystal planes, graphitic structure.

FT-IR spectra were recorded to evaluate the functional groups on the activated carbon and are shown in Fig. 2. The peak around 3440 cm^{-1} is the O–H stretching of the hydroxyl functional groups [11], and the adsorption peak at 1600 cm^{-1} is aromatic C=C stretching vibrations [12]. The peak at 1440 cm^{-1} is for aliphatic C–H bending vibrations [13], and the peak at 3300 cm^{-1} is the IR adsorption peak of alkyne C–H vibration [14]. The peaks appeared at activated carbons tend to decrease as amounts of NaOH increase. This result indicates that cleaning effect occurred on the surface of material during activation process.

Characterization of the porous structure

The N_2 adsorption isotherms of the samples are presented in Fig. 3. Non-activated sample Pitch shows the quite low N_2 adsorption relatively, showing the non-developed pore structure. The isotherm of AC1 shows type I showing the characteristic of micropores according to IUPAC classification [15,16]. The others show type I at relatively low pressures (less than 0.1 P/P$_0$), and simultaneously appear some mesopores behavior of type IV over the range of the relatively high pressures. The isotherms of the samples except AC1 increase remarkably in lower than 0.4 P/P$_o$, and show a typical hysteresis loop in the intermediate relative pressure range. These results suggest that the samples typically have bottleneck shaped pores containing both the micropore and mesopore region, it is also show in SEM image of Fig. 4.

As shown in Table 1, the total pore volume and specific surface area increased gradually with higher amount of activation agent, NaOH. The AC6 has the highest values for specific surface area and total pore volume of 1409 $m^2 g^{-1}$ and 0.79 $cm^3 g^{-1}$, respectively.
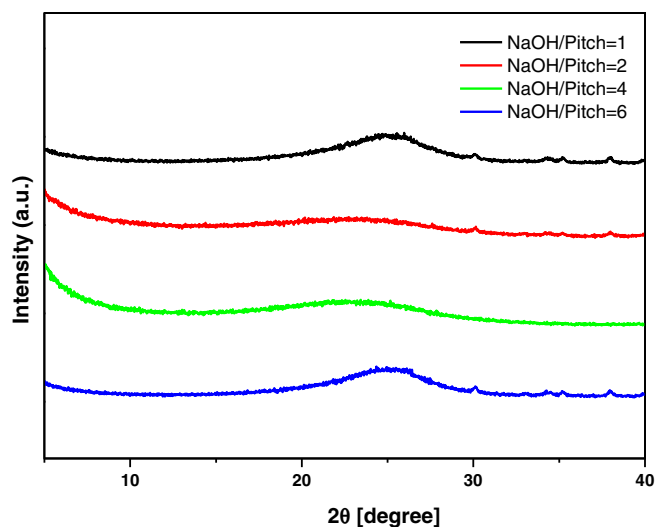

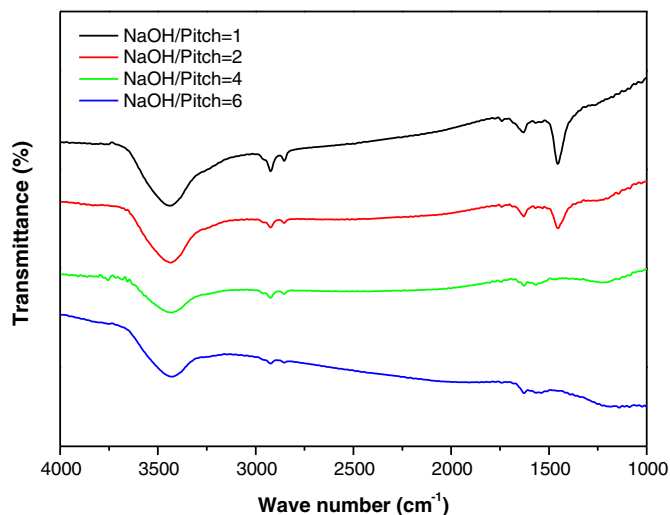Fig. 1. X-ray diffraction of the pitch-based activated carbon by NaOH of various amounts.

Fig. 2. FT-IR spectra of activated carbon by NaOH of various amounts.

Fig. 3. Nitrogen adsorption/desorption isotherms for activated carbon samples.

In EDLCs, the surface area of the electrode is an important parameter. Also, specific capacitance is affected by how easily the ion of electrolyte can access the pores of the electrode materials based on pore structure.

For decades, the several results have been published for optimum pore size based on efficient capacitor: (i) less than 1 nm in dimension [17], (ii) mesopores larger than electrolyte ions [18,19], (iii) larger than around 0.5 nm, (iv) around 0.7 nm [20].

In this paper, the pore size effects were studied based on capacitor performance. The pore size distributions of the activated carbon samples were compared in detail, as shown in Fig. 5. The samples developed micropores and small mesopores in 2–5 nm. The ultrafine micropores (<1 nm) with pore width peaks at 0.6 and 0.8 nm and micropores (1–2 nm) with a maximum peak at 1.2 nm provide ion-accessible surface which play a important role for the formation of an electrical double layer capacitor [17]. In addition, the small mesopores (2–5 nm) provide a channel for fast ion transport and a low resistance for charge transfer [21].
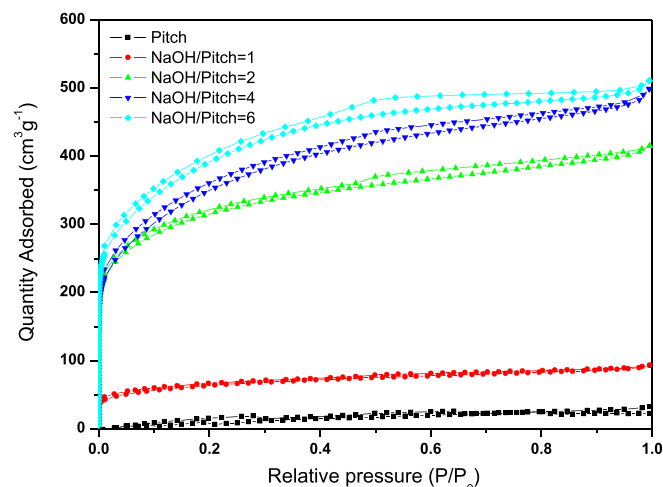
Electrochemical properties

Cyclic voltammetry

In order to investigate the effect of pore distribution on the electrochemical properties of the pitch-based activated carbon electrode, the performance of the prepared electrode was tested by cyclic voltammograms (CV). The specific capacitance of the samples can be calculated according to the equation $C = \int I dv / vm\Delta V$, where I is the response current density (A cm^{-2}), v is the potential scan rate (V s^{-1}), ΔV is the difference between the highest and lowest potential (V) and m is the mass of the composite in the electrodes (g) [22,23]. The calculated specific capacitances of the electrodes are shown in Table 2. The AC4 achieved the highest capacitance of 287.43 F g^{-1} at scan rate 50 mV s^{-1}. According to Chen and Xue the Ni foam could provide capacitances in alkaline electrolytes [24]. Specific capacitance of Ni foam at scan rate 50 mV s^{-1} in 2 M KOH has 0.45 F g^{-1}. It is essential to consider the contribution from the Ni foam in order to get correct specific capacitance. However, in this study, it was not calculated
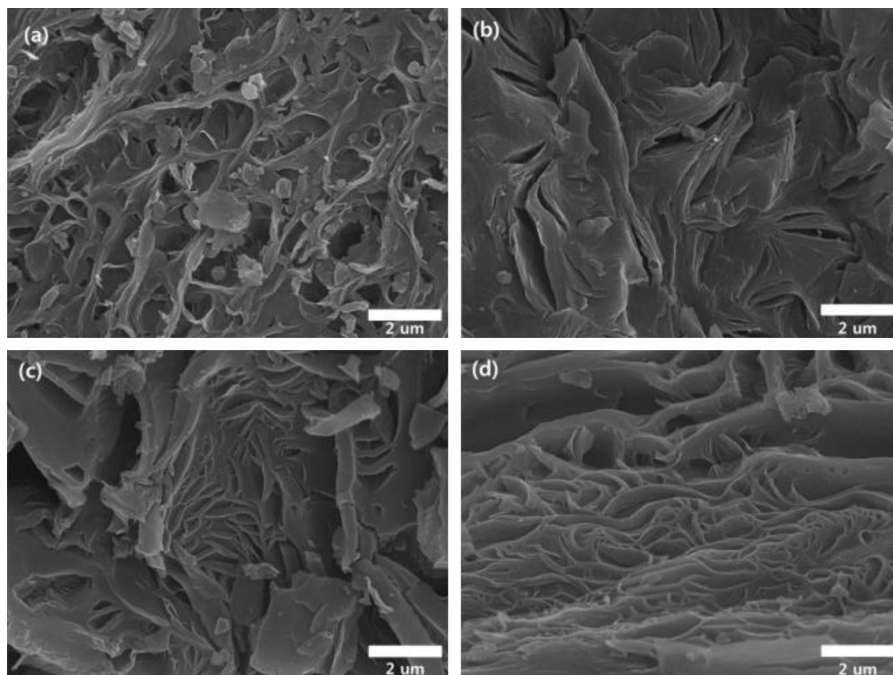

Fig. 4. SEM images of NaOH-activated carbon that the weight ratio of NaOH and Pitch is (a) 1:1, (b) 2:1, (c) 4:1, and (d) 6:1.

Table 1
Structure characterizations of activated carbon samples.

Samples	S_{BET}[a] $(m^2\,g^{-1})$	S_{meso}[b] $(m^2\,g^{-1})$	V_{total}[c] $(cm^3\,g^{-1})$	V_{micro}[d] $(cm^3\,g^{-1})$	V_{meso}[e] $(cm^3\,g^{-1})$
AC1	230.05	36.77	0.1438	0.0811	0.0623
AC2	1149.2	196.0	0.6433	0.4090	0.2179
AC4	1262.8	227.7	0.7731	0.4231	0.3324
AC6	1409.7	217.8	0.7915	0.4930	0.2793

[a] S_{BET}: BET specific surface area.
[b] S_{meso}: mesopore specific surface area.
[c] V_{total}: total pore volume.
[d] V_{micro}: micropore volume.
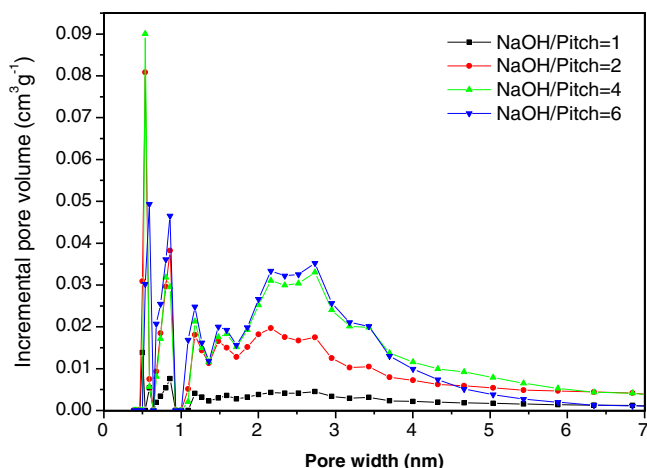[e] V_{meso}: mesopore volume.

Fig. 5. Pore size distribution of activated carbon samples.

Table 2
The specific capacitances of the samples at scan rate 50 mV s^{-1}.

Sample	Reaction condition	NaOH/pitch	Yield (%)	Capacitance $(F\,g^{-1})$
AC1	750 °C, 3 h	1	69.1	66
AC2		2	67	247.94
AC4		4	39.31	287.43
AC6		6	22.59	264.1

separately because it is very marginal value in this experimental condition.

It is presented that CV curves of pitch-based activated carbon having the highest capacity (AC4) at various scan rates in the potential range of −0.9–0.0 V (vs. SCE) in Fig. 6. The CV curves exhibit a good rectangular shape, representing energy storage by an electrical double layer mechanism.

Fig. 7 shows that the specific capacitance of samples of various ratio at different scan rate. Compared to AC4 and AC2, it is noted that AC4 having much mesopore presents the higher specific capacitance and the small decrease in specific capacitance with increasing scan rate. The results reveal that such mesoporous material has a large electroactive area on the surface layer, and it is not only shortens diffusion paths for high rate charge–discharge, but also indicates excellent ion transportation, which can be mainly attributed to the mesopores.

Galvanostatic charge–discharge curve

The charge–discharge behavior of electrode was measured between −0.9 and 0.0 V (vs. SCE) at current density of 1 A g^{-1}, which is displayed in Fig. 8. The linear symmetric profiles indicate that the pitch-based activated carbon electrode has a high
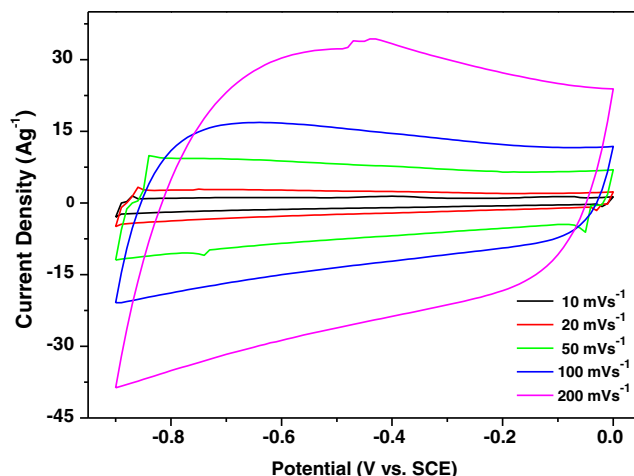

Fig. 6. Cycle voltammetry (CV) curves of pitch-based activated carbon at various scan rates (weight ratio of NaOH and Pitch is 4:1).
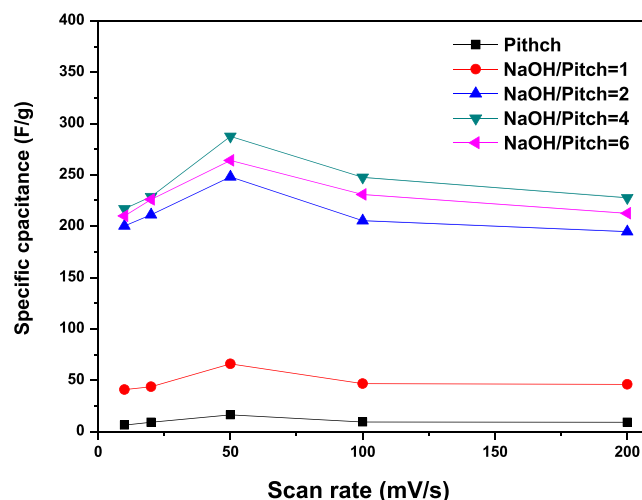

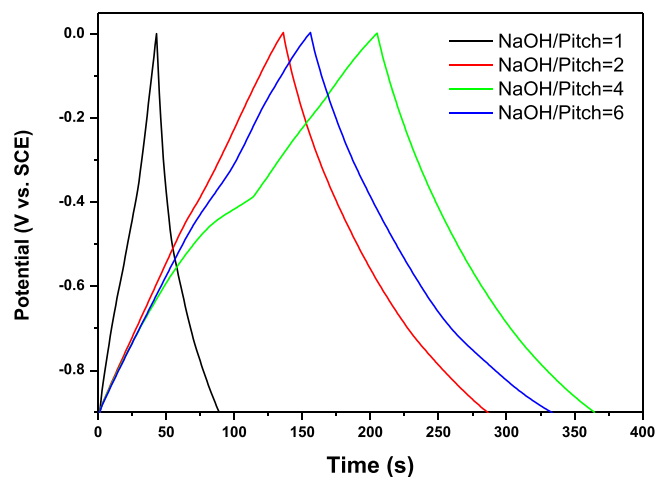**Fig. 7.** A change of specific capacitance of the samples at different scan rates.

Fig. 8. GV charge–discharge curves of NaOH-activated pitch of various weight ratio at the same current density of 1 A g^{-1}.

Coulombic efficiency and excellent reversibility. The value of specific capacitance (C_s) of the electrode is calculated according to discharge part using the equation: $C_s = I\Delta t/(m\,\Delta V)$, where I is the discharge current, Δt is the discharge time, and ΔV represents for
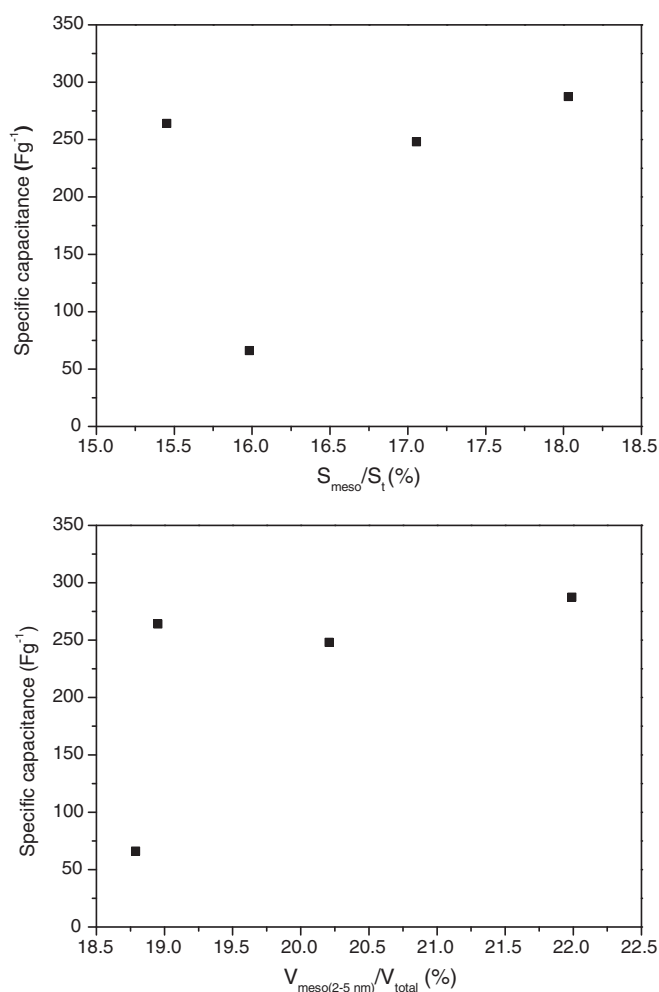
Fig. 9. Relation between specific capacitance and mesopore fraction for activated carbons.

Fig. 10. Specific capacitance plots as a function (a) $S_{meso}/S_t(\%) * S_c$ and (b) $V_{meso}/V_t(\%) * V_c$.

the potential difference during the discharge. Here we take the potential range (-0.9–0.0 V) to calculate the C_s and m is the mass of electrochemical active material in the electrode. The specific capacitance of the samples is 52.22, 167.78, 197.78, and 177.78 F g^{-1} at the current density 1 A g^{-1} for AC1, AC2, AC4, and AC6, respectively.

To further evaluate the specific capacitance of AC4 electrode, we can calculate the average energy density of the electrode from the galvanostatic charge–discharge data using the following equations [25]:

$$E = 1/2C_{s*}(\Delta V)^2$$

where E is the average energy density of the electrode (Wh kg^{-1}), C_s is the specific capacitance of the electrode (F g^{-1}), and ΔV is the potential range. The calculated average energy density of the electrodes is 0.888, 9.17, 16.34, and 11.16 Wh kg^{-1}, respectively, AC1, AC2, AC4, and AC6.

Discussion

As it is known, the specific surface area and pore structure of materials are significant in determining the EDLC performance of electrode based on activated carbon [26]. According to Tables 1 and 2, the specific capacitance of the AC4 is higher than that of AC6 although AC6 has the larger surface area and pore volume. This
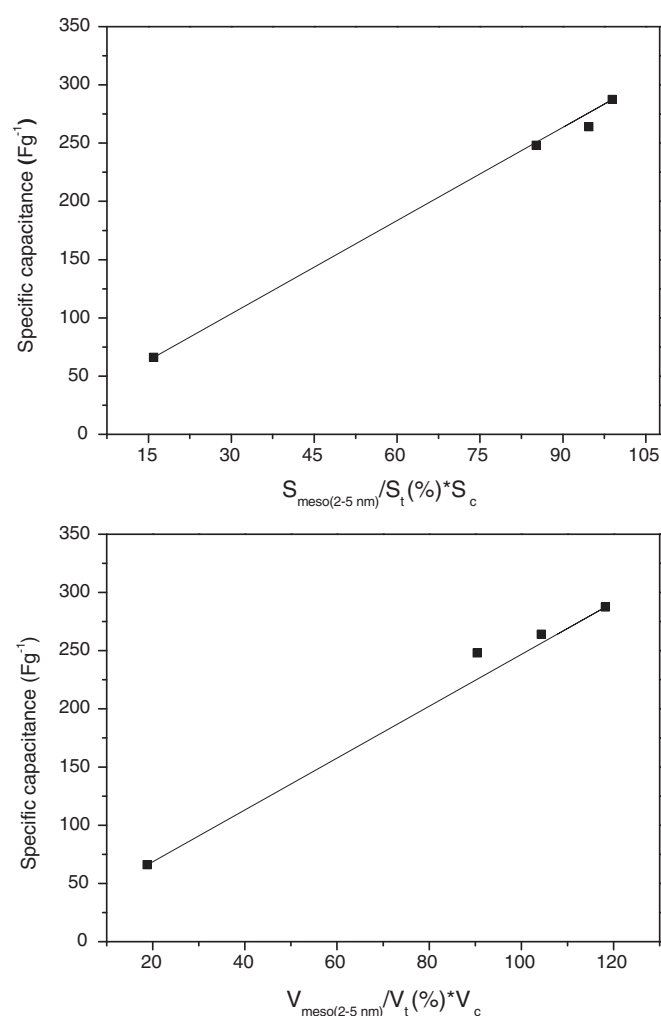
interesting result implies that the specific capacitance of EDLC is affected not merely total specific surface area and total pore volume but also other specific factors such as pore size distribution and functional group.

Fig. 9 shows how the small mesopore (2–5 nm) contribution to porous structure (S_{meso}/S_t and V_{meso}/V_t) affects the specific capacitance of the activated carbon. A lack of linearity between those two parameters suggests that the others factor with mesopore fraction influence on electrochemical performance of EDLC.

The lines shown in Fig. 10 can get from the following relation:

$$Cs = 266.82(S_{meso}/S_t(\%) * S_c) + 23.36$$

$$Cs = 2.27(V_{meso}/V_t(\%) * V_c) + 24.17$$

where S_c and V_c are, respectively, the correction value of surface area and total pore volume. It is calculated and multiplied by the small mesopore fraction to reflect the relative amount of the mesopore. The data obtained through experiment in this study marked with dots, and the dots are well fitted to the proposed line. It means that the specific capacitance affects both small mesopore fraction and relative amount. Therefore, the specific capacitance of EDLC is decided on proper ratio and amount of mesopore.

Conclusions

The pitch, the residue obtained after pyrolysis of distillation of tar, was recycled as electrode materials for EDLCs following a NaOH activation process. The pitch-based activated carbon had a large surface area and micro-, mesoporous structures. The S_{BET} and V_{total} of the ACs increased with the activation agent to precursor ratio. A EDLC using the AC4 as the electrode showed superior capacitive behavior. The gravimetric capacitance was 197.78 F g^{-1} at a current density of 0.1 A g^{-1}, and exhibited excellent rate capability. Furthermore, the electrode using AC4 shows the high energy density, 16.34 Wh kg^{-1}. These outstanding results are attributed to the moderate amount and fraction of small mesopore (2–5 nm).

The AC from coal tar pitch not only can achieve high capacity but also can provide a continuous three dimensional pore network for fast ionic motion, resulting in high energy density. The pitch-based activated carbon exhibits great potential for applications in energy storage. Additionally, it is meaningful material from economic and eco-friendly point of view.

References

[1] E. Fitzer, K.H. Köchling, H. Marsh, Pure Appl. Chem. 67 (1995) 473–506.
[2] H. Marsh, E.A. Heintz, F. Rodriguez-Reinoso, Introduction to Carbon Technologies, Universidad de Alicante, Alicante, Spain, 1997.
[3] V.G. Rocha, M. Granda, R. Santamaría, C. Blanco, E.I. Diestre, R. Menéndez, J. Anal. Appl. Pyrolysis 73 (2005) 276–283.
[4] V. Slovák, P. Susàk, J. Anal. Appl. Pyrolysis 72 (2000) 249–252.
[5] S. Mitani, S. Lee, S. Yoon, Y. Korai, I. Mochida, J. Power Sources 133 (2004) 298–301.
[6] G. Grazyna, M. Jacek, L. Ewa, L. Grzegorz, F. Elzbieta, Electrochim. Acta 50 (2005) 1197–1206.
[7] T. Weng, H. Teng, J. Electrochem. Soc. 148 (2001) A368–A373.
[8] D. Lozano-Castello, D. Cazorla-Amoros, A. Linares-Solano, S. Shi-raishi, H. Kurihara, A. Oya, Carbon 41 (2003) 1765–1775.
[9] H. Shi, Electrochim. Acta 41 (1996) 1633–1639.
[10] D. Qu, H. Shi, J. Power Sources 74 (1998) 99–107.
[11] Y. Guo, Z. Shi, M. Chen, C. Wang, J. Power Sources 252 (2014) 235–243.
[12] M. Acik, C. Mattevi, C. Gong, G. Lee, K. Cho, M. Chhowalla, Y.J. Chabal, ACS Nano 4 (2010) 5861–5868.
[13] H.M. Zhu, J.H. Yan, X.G. Jiang, Y.E. Lai, K.F. Cen, J. Hazard. Mater. 153 (2008) 670–676.
[14] S. Kim, K. Lee, Chem. Phys. Lett. 400 (2004) 253–257.
[15] J.B. Condon, Surface Area and Porosity Determinations by Physisorption: Measurements and Theory, Elsevier, The Netherlands, 2006.
[16] H.-R. Yu, S. Cho, M.-J. Jung, Y.-S. Lee, Microporous Mesoporous Mater. 172 (2013) 131–135.
[17] J. Chmiola, G. Yushin, Y. Gogotsi, C. Portet, P. Simon, P.L. Taberna, Science 313 (2006) 1760–1763.
[18] R.H. Baughman, A.A. Zakhidov, W.A. de Heer, Science 297 (2002) 787–792.
[19] E. Frackowiak, J. Braz. Chem. Soc. 17 (2006) 1074–1082.
[20] E. Raymundo-Piñero, K. Kierzek, J. Machnikowski, F. Béguin, Carbon 44 (2006) 2498–2507.
[21] D.W. Wang, F. Li, M. Liu, G.Q. Lu, H.M. Cheng, Angew. Chem. 120 (2008) 379–382.
[22] S. Park, S. Kim, Electrochim. Acta 89 (2013) 516–522.
[23] Q. Zhang, Y. Li, Y. Feng, W. Feng, Electrochim. Acta 90 (2012) 95–100.
[24] K. Chen, D. Xue, J. Nanoeng. Nanomanuf. 4 (2014) 55.
[25] J. Yan, J. Liu, Z. Fan, T. Wei, L. Zhang, Carbon 50 (2012) 2179–2188.
[26] B. Xu, F. Wu, R. Chen, G. Cao, S. Chen, Y. Yang, J. Power Sources 195 (2010) 2118–2124.